Investigating the influence of micro-and nanoplastics on CaLu-3 cells using a lung-on-chip microfluidic device

By Sanne van Kooten, s2594323
Supervision by Prof. Dr. Ir. S. le Gac
Daily supervision by L. Mol
External supervision by Dr. K. Broersen
University of Twente, Biomedical Engineering
AMBER
January 26, 2024

Since the 1950s, plastics have been used extensively for all kinds of purposes, like food packaging and clothing. This has resulted in a lot of plastic waste, of which 90% is not properly disposed. Therefore these plastics end up in landfills and environments, resulting in the formation of micro- and nanoplastics (MNPs) through degradation due to the environment. Humans come into contact with these MNPs by consuming food and drinks contaminated with MNPs, or by inhaling air containing MNPs. There is little known information about MNP exposure in the lungs as there are currently no models that accurately represent the in vivo environment of the lungs. This research focuses on the influence of MNPs on lung epithelial cells by using a novel lung-on-a-chip system in comparison with the Transwell system, the standard model. This was done by firstly investigating the optimal cell seeding density within a well plate and a static lung-on-a-chip (StatLoC) covered with Gelatin methacrylate and comparing the difference in cell characteristics. This is done with the goal of optimizing cell culturing within the StatLoC, which will be compared to the Transwell system. Finally, the influence of micro-and nanoplastics is studied by adding MNPs to the Transwell and StatLoC systems and comparing the results. Results show that the optimal cell seeding density within the StatLoC system is $5*10^5$ cells/cm^2 and that MNPs with 0.2 µm diameter have the greatest potential of crossing cell membranes. However, these results have limited relevance as the StatLoC chip needs more optimization, specifically regarding Gelatin Methacrylate fragmentation and detachment, before it can reliably be used to replace the Transwell system for lung-on-chip research.

1. Introduction

Plastic, a synthetic material consisting of polymers, was introduced in 1907. Since then, the material has been used all over the world in large numbers for applications like food packaging and clothing. All plastics consist of long carbon chains, which do not compost naturally and thus need to be disposed of properly. However, only 9% of all plastics is properly disposed of, the rest of this end up in landfills and the environment [1]. Due to a variety of factors like mechanical abrasion and UV exposure, these plastics break down into micro- and nanoplastics (MNPs) which are particles ranging in size from 5 mm to under a micrometer [2]. These plastics invade marine and terrestrial environments and the life within these regions, humans included [3].

Micro- and nanoplastics can be assorted in two categories, primary and secondary MNPs. Primary MNPs end up in the environment in micro- or nanoscale form, while secondary MNPs are created by fragmentation of plastics [3]. Primary MNPs consist of pellets and beads and are found very little (<5%), while secondary MNPs consist of fragments, films and fibers which are detected the most (90%) [4]. On average, humans ingest 5 grams of MNPs per person per week, which is about as much as a creditcard [3].

These MNPs can then be internalized by cells through passive and active targeting, passive targeting being transport across membranes without ATP consumption and active with ATP consumption. When internalized, MNPs can cause cell death by promoting damage on membrane structures

[5]. They can also transport toxic substances which can cause diseases of the endocrine and reproductive system, cause inflammation, oxidative stress and neurotoxicity [6]

However, studying the effects that these MNPs may have on the human body is difficult, as existing models have limited relevance due to insufficient simulation of the in vivo situation. To be able to better understand the interactions between MNPs and the human body, a lung-on-a-chip system is being developed, which will be optimized and tested with MNPs to study the effects.

The current gold standard for lung research on a cellular level is the Transwell system. A Transwell consists of inserts that can be positioned in wells to create an apical and basolateral compartment. A porous membrane separates these compartments and supports formation of a confluent cell layer. In this way, transport across cellular barriers can be measured [7]. For these systems, the membrane choice is important as it has to allow the transported particles to pass through the membrane, otherwise they will accumulate at the membrane. Transwells also enable air-liquid interface (ALI) culturing, which aim is to better enable airway cell culturing by simulating the in vivo conditions.

However, there are a few shortcomings in the Transwell system which make simulating the in vivo lung conditions more difficult. The Transwell inserts are not biomimetic, agglomeration occurs at the membrane and the membrane in the inserts is too stiff and not curved [7]. To be able to improve upon these shortcomings a new chip was developed, the static lung-on-a-chip (StatLoC).

To study how MNPs influence lung epithelial cells in a lung-on-a-chip device compared to lung epithelial cells cultured in transwell systems, the StatLoC must first be optimized. The correct seeding density must be found in a well plate with Gelatin Methacrylate (GelMA) and in the StatLoC system and differences in cell morphology between the StatLoC and Transwell system must be investigated. Lastly, the influence of MNPs on lung epithelial cells needs to be determined in the StatLoC and Transwell system.

The static lung-on-a-chip can be seen in Figure 1 and consists of 2 parts, of which the apical half has 2 inlets to allow for medium to be added into the chip. The basolateral part has 3 important structures, of which the first is a circular channel in which the medium is supplied. Inside this, there is a circular row of pillars, which serve the purpose of separating the medium and the GelMA just enough so that they are still in contact to allow diffusion. In this way, medium can be supplied to the cells through the GelMA, in which way ALI culture can be realised when the medium on the apical side is removed. Inside of this circular row of pillars there is an area with grooved hydrogel on which the cells will be cultured. The grooved hydrogel is made with a stamp and functions to improve the biomimetic and as a way to simulate the smallest brochioles, as the grooves have a diameter of approximately 400 µm [8].

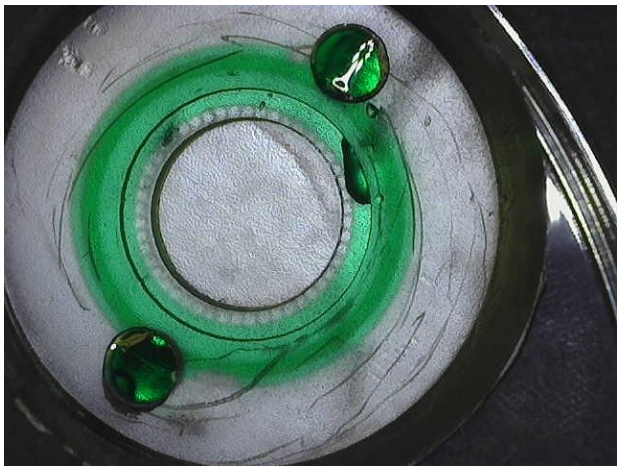

Figure 1: StatLoC. The medium channel is filled with green food colouring, while the culture chamber can be seen in the middle. The pillars separating the culture chamber and medium channel can be seen holding the green liquid in the medium channel.

The cells that will be used are CaLu-3 cells, an epithelial cell line derived from a submucosal glands from a lung

adenocarcinoma. These cells are widely used in airway epithelial barrier research because CaLu-3 cells forms tight junctions and good monolayers, which are essential for the formation of an epithelial barrier [9]. The precise structure these cells form depends on the culture method; when cultured at a liquid-liquid interface, CaLu-3 cells form a simple cuboid epithelium, while at an air-liquid interface a pseudostratified columnar epithelium is formed which resembles the native bronchiolar epithelium [10].

This article describes the influence of micro- and nanoplastics on lung epithelial cells, which is researched with a static lung-on-a-chip system in comparison to the Transwell system. This was done to improve the shortcomings of the Transwell system. It introduces experimental methods for studying the optimal seeding density within the StatLoC system combined with GelMA, methods for comparing the performance between the StatLoC and Transwell system and methods for studying the MNP uptake by CaLu-3 cells. These methods enable the study of the effect of GelMA on CaLu-3 cell growth, the difference in protein expression in the StatLoC and Transwell systems and protein expression, viability and translocation of MNPs in both systems.

2. Materials and methods

2.1 Cell culturing

Cells used are CaLu-3 cells, from passage 22 until 35. Cells were cultured using Roswell Park Memorial Institute medium (RPMI, ThermoFisher) supplemented with 10% fetal bovine serum (Sigma Aldrich), 1% penicillin-streptomycin (Gibco), 1% GlutaMAX (Gibco) and 1mM sodium pyruvate (Gibco). The medium is refreshed 3 times per week and the cells are passaged once every week.

2.2 Production of the StatLoCs and stamps

Polydimethylsiloxane (PDMS) is an elastomer widely used in chip fabrication because of its biocompatibility and chemical stability [11]. PDMS was made by mixing a PDMS pre-polymer (Sylgard) with a PDMS crosslinker (Sylgard) in a 10:1 weight ratio. The PDMS was poured into the previously printed 3D-printed molds and dessicated for 30 minutes at -0.08 MPa. When dessicated, the molds were placed into an oven at 65 °C for at least an hour, sometimes longer to a maximum of overnight. The chip halves were then removed from the molds and bonded. After this, the chips were placed inside an oven at 65 °C again overnight to further stimulate bonding.

The PDMS stamps to create the topological grooves are made from 10:1 PDMS following the same methodology. The stamps were then deposited into a 1% w/v bovine serum albumin solution (Sigma Aldrich) for at least 30 minutes to prevent the GelMA from sticking to them.

2.3 Production of the GelMA and GelMA layer in wells and StatLoCs

Gelatin Methacrylate (GelMA) hydrogel consisted of 0.5% w/v Irgacure 2959 (Sigma Aldrich) and 7% w/v Gelatin Methacryloyl (Sigma Aldrich) dissolved in PBS (Sigma Aldrich). The StatLoCs are treated for application of the GelMA by applying a polydopamine (Sigma Aldrich) coating in 2mg/mL Tris-HCl buffer for 1 hour. This was done to ensure bonding of the GelMA to the chip.

After coating the culture chamber with a polydopamine solution, the GelMA was added and the stamps were placed on top. The StatLoCs were then refrigerated for 5 minutes, cured under a 365 nm UV light for 2 minutes at an intensity of 6 mW/cm^2 and incubated at room temperature for 10 minutes. After this, the stamps were removed.

2.4 Comparison cell seeding density

The optimal cell seeding density was determined using a 48-well plate and StatLoCs. The 48-well plate was used to determine the seeding density on the

GelMA, while the StatLoC chips were used to determine the cell seeding density on the grooved GelMA. The 48-well plate contained 15 different culture conditions, with cell seeding densities ranging from $4*10^3$ cells/cm^2 to $5*10^6$ cells/cm^2 , water with cells and medium without cells as negative controls. All conditions were tested in triplo.

The seeding densities tested in the StatLoC chips were based on the optimal seeding density found in the 48-well plate containing GelMA. These conditions are $2*10^5$ cells/cm^2 , $4*10^5$ cells/cm^2 , $5*10^5$ cells/cm^2 , $8*10^5$ cells/cm^2 , medium without cells and cells in water as negative controls. All conditions were tested in triplo.

To compare cell characteristics in the 48-well plate, morphology assessments and time to confluency were taken into account.

2.5 Comparison cell characteristics and morphology of the StatLoC and Transwell

The proliferation rate and morphology of Calu-3 cells cultured in StatLoCs was compared to those cultured in Transwell inserts. For this, the following seeding densities were used: $2*10^5$, $4*10^5$, $5*10^5$, $8*10^5$ cells/cm^2 . After the cells were seeded onto the inserts and the chips, they were cultured for 7 days, changing the medium every 3 times per week. After 7 days, an airlift is performed and air-liquid interface (ALI) culturing was started. After a week, cells were fixed using 10% formalin (Qpath) and a 4',6-diamidino-2-phenylindole (DAPI) and zona occludens-1 (ZO-1) tight junction staining were performed. The 1:100 DAPI in PBS staining was incubated for 15 minutes while the 1:200 anti-ZO-1 in 1% w/v BSA

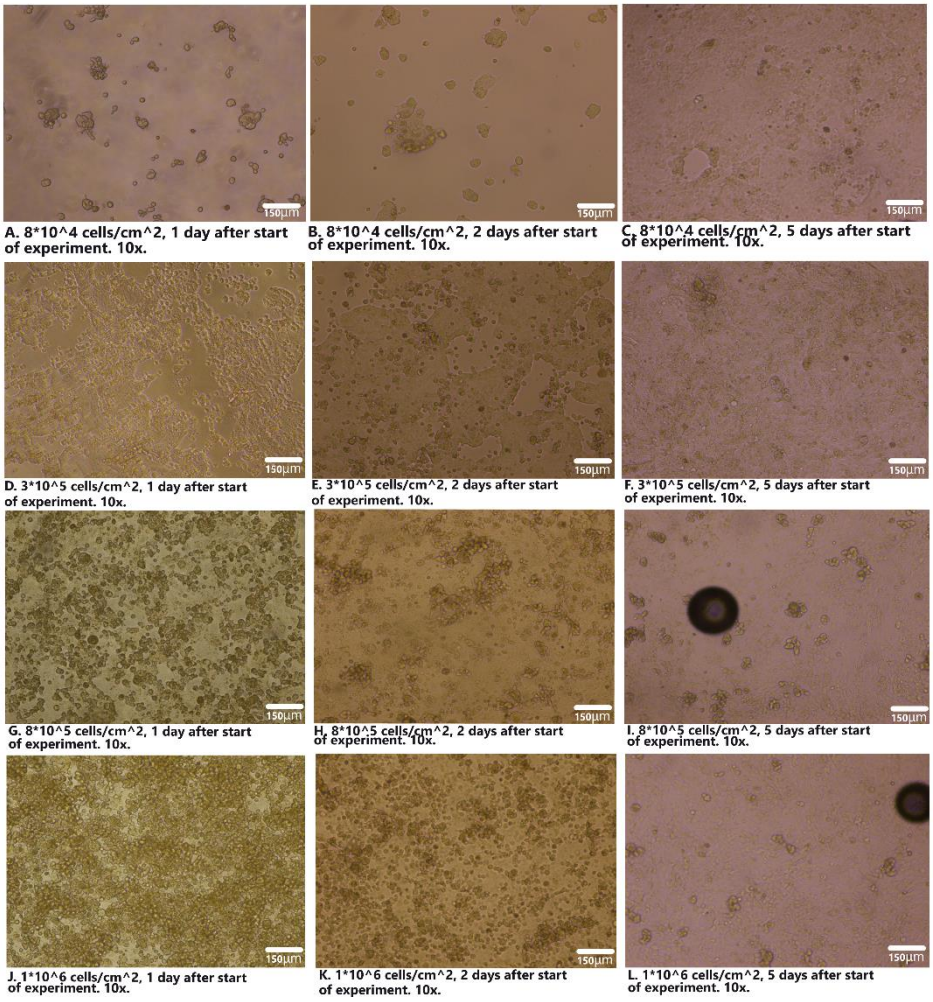

Figure 2: Results of the cell seeding density wellsplate experiment. A to C is $8*10^4$ cells/cm^2, D to F is $3*10^5$ cells/cm^2, G to I is $8*10^5$ cells/cm^2 and J to L is $1*10^6$ cells/cm^2.

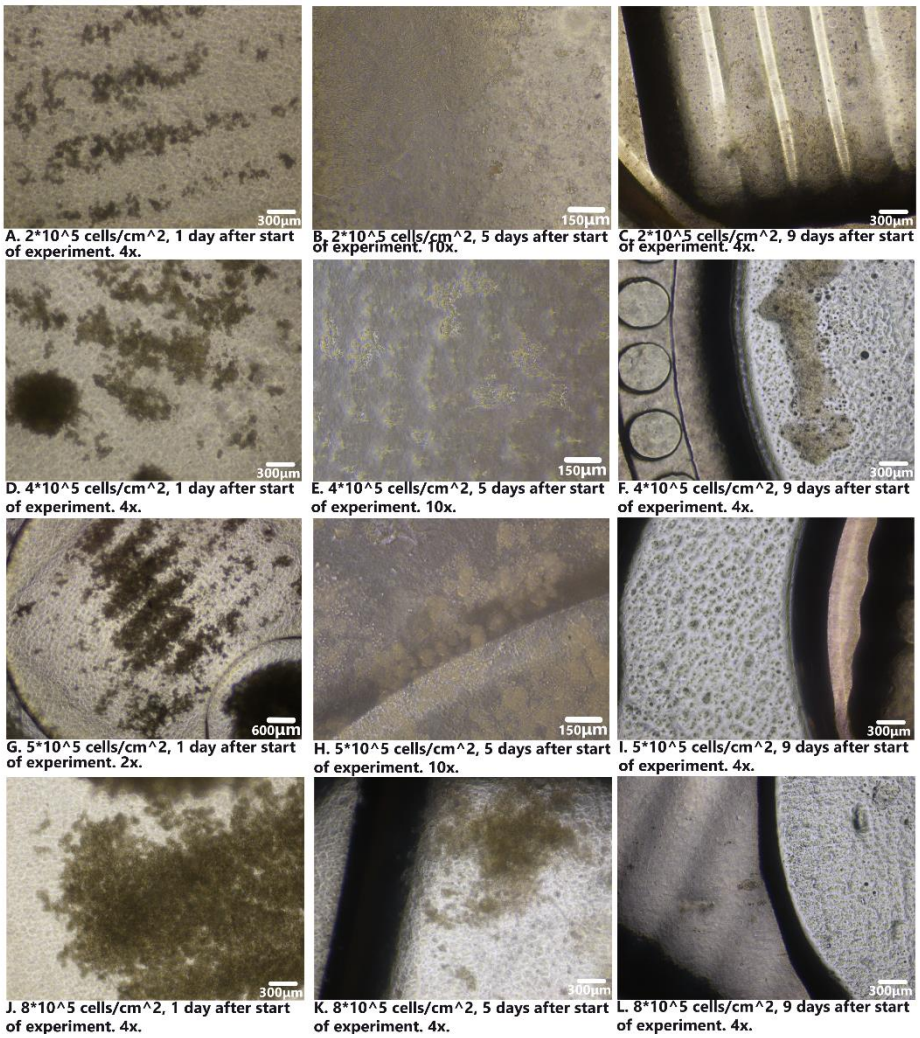

*Figure 3: Results of the cell seeding density StatLoC experiment. A to C is 2*10^5 cells/cm^2, D to F is 4*10^5 cells/cm^2, G to I is 5*10^5 cells/cm^2 and J to L is 8*10^5 cells/cm^2.*

was incubated overnight. The 1:200 secondary antibody in 1% w/v BSA was incubated for an hour. These staining results were analyzed using the Zeiss LSM880 confocal microscope and processed using Fiji.

2.6 Uptake and translocation studies

To assess uptake and translocation of MNPs by the CaLu-3 cells, the cells are cultured with a cell seeding density of 5*10^5 cells/cm^2 . After the cells were seeded onto the inserts and the chips, they were cultured for 4 days, changing the medium 3 times per week. After 4 days, an airlift is performed and air-liquid interface (ALI) culturing was started. After 4 days of ALI culturing, the polystyrene MNPs (Bangs Laboratories) are added to the apical side of the cells and incubated for 24 hours in 4 different MNP types, namely 0.2 µm diameter, 0.5 µm diameter, 1 µm diameter and mixed MNPs. The micro- and nanoplastics utilize dragon green as a fluorophore and are shaped like beads. The mixed MNPs consisted of an even volume distribution of the 3 different sizes. All types were done with the same concentration of 100 µg/mL.

After this, 2/3 of the cells were fixated while 1/3 of the cells were stained with a live dead staining. Once fixated, the DAPI, phalloidin and ZO-1 tight-junction staining and morphology assessment were carried out. Uptake and translocation were assessed by confocal imaging using the Zeiss LSM880 and processed using Fiji.

3. Results

3.1 Comparison cell seeding density well plate

The cell seeding density experiment is performed to optimize the CaLu-3 cell seeding density on GelMA. To find the optimal cell seeding density, there must first be a definition for optimal in these circumstances. In this case, the optimal seeding density is when confluency is reached within four days and as little multiple layers as possible are formed. Because there were not enough cells to perform all conditions, only 4 were chosen. These conditions are $8*10^4$ cells/cm^2 , $3*10^5$ cells/cm^2 , $8*10^5$ cells/cm^2 and $1*10^6$ cells/cm^2 .

As can be seen in Figure 2 ABC, the cell seeding density of $8*10^4$ cells/cm^2 gives rise to many small clusters of cells, which do not reach full confluency within 4 days. The cells have a more stretched morphology when compared to the other conditions.

When looking at the cells in figure 2 GHI and JKL, it can be seen that $8*10^5$ cells/cm^2 and $1*10^6$ cells/cm^2 are too high, as confluency is reached within 2 days after the start of the experiment. It can also be seen that multiple layers have started forming at day one and the cell morphology is also more circular in comparison to the conditions seen in Figure 2 ABC and DEF. Lastly, when looking at the cells in Figure 2 DEF it can be seen that the cell seeding density of $3*10^5$ cells/cm^2 does not reach full confluency at day 5. The condition also formed multiple layers. From this, it can be concluded that $3*10^5$ cells/cm^2 is the best cell seeding density within a well plate covered with GelMA, but it is not optimal.

3.2 Comparison cell seeding density StatLoC

The cell seeding density experiment is performed to optimize the CaLu-3 cell seeding density on grooved GelMA in the StatLoCs. For this experiment, the same criteria for the optimal cell seeding density are used as in section 3.1. With these chips, an airlift has been performed at day 5 to facilitate air-liquid interface culturing.

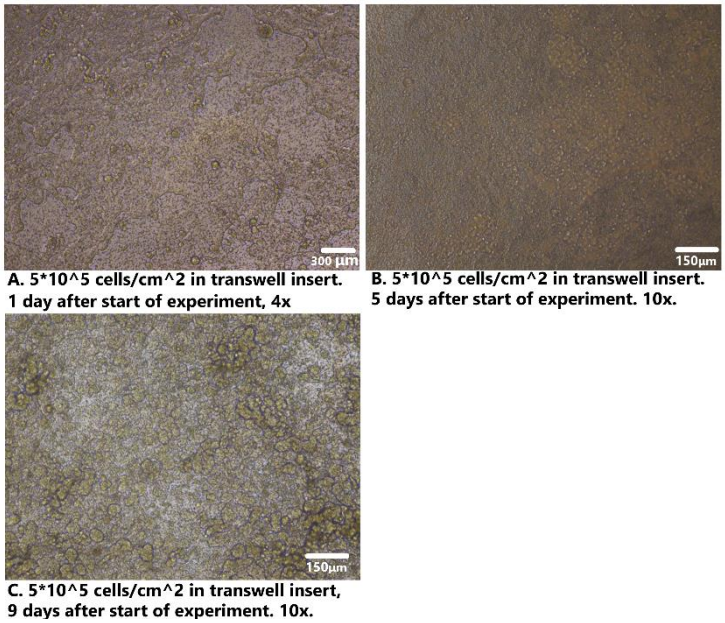

Figure 4: Results of the cell seeding in Transwell inserts. A, B and C show a cell seeding density of $5*10^5$ cells/cm^2.

When comparing the results of the cell seeding densities in the StatLoCs, it can be noted that the final confluency of the cell seeding densities in the chip differ by a lot, even in chips within the same condition. Furthermore, an unusual cell morphology can be seen in Figure 3 FIL, where the cells in the StatLoCs are shaped like droplets. From Figure 3 ABC, it can be seen that the final confluency for this condition is approximately 50% and the cell morphology is rounded. Furthermore, in some areas cells have formed multiple layers, despite not reaching confluency. For the condition shown in Figure 3 DEF, the confluency of the chips is about 70%. Similar to the condition containing $2*10^5$ cells/cm^2 , the cells have started to form multiple layers in some regions while not reaching full confluency. The same can be said for the condition in Figure 3 GHI, as the confluency is about 70% and multiple layers have started to form in some areas. Lastly, the condition in Figure 3 JKL in general developed to be overconfluent in some chips and nearing

100% confluency in the rest. The cell morphology here was smaller in comparison to the other conditions.

One thing to note when looking at Figure 3, is that barely any cells grew on top of the GelMA. This can be seen especially well in Figure 3 L, where there are no cells on the GelMA while there are plenty of cells at the bottom of the culture chamber of the chip. From this, we can conclude that $5*10^5$ cells/cm^2 is the optimal cell seeding density within StatLoCs with grooved GelMA.

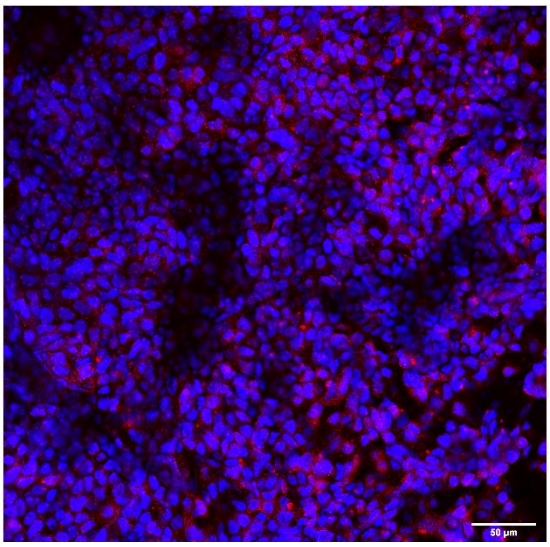

Figure 5: Result of the Transwell staining. Red is ZO-1 protein, blue is DAPI. 20x.

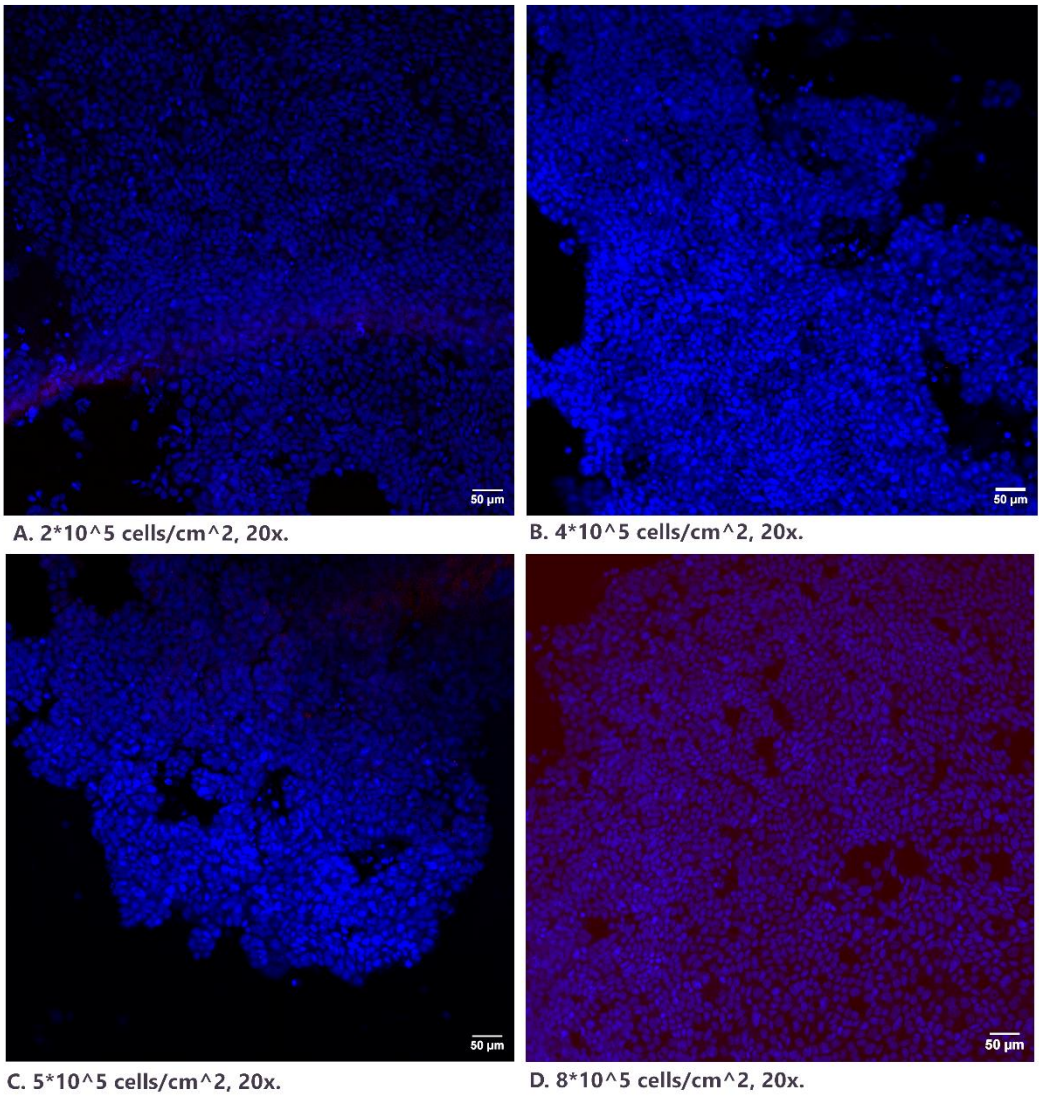

Figure 6: Results of the StatLoC staining. Red is ZO-1 protein, blue is DAPI. No red staining can be seen. 20x

3.3 Comparison of the cell characteristics and morphology between the StatLoC and Transwell

The comparison between the StatLoCs and Transwells is done to determine any differences in cell morphology and characteristics. From this, the performance of the StatLoCs can be seen compared to the Transwells. To compare the two systems, three criteria will be used to determine the performance of both methods. These criteria consist of confluency being reached within four days, a monolayer being formed with as little multiple layers as possible. With these chips and inserts, an airlift has been performed at day 5 to facilitate air-liquid interface culturing.

In the cells in Figure 4, it can be seen that full confluency has been reached at day five. At day 9, the cells have grown multiple layers and are thus overconfluent. The cell morphology of these cells are rounded and quite large in comparison to the cells of Figures 2 and 3.

When comparing the cells from the StatLoCs and Transwells in Figure 3 and 4, it can be seen that both have formed multiple cell layers in all chips/inserts. The difference here is that in the StatLoCs confluency has

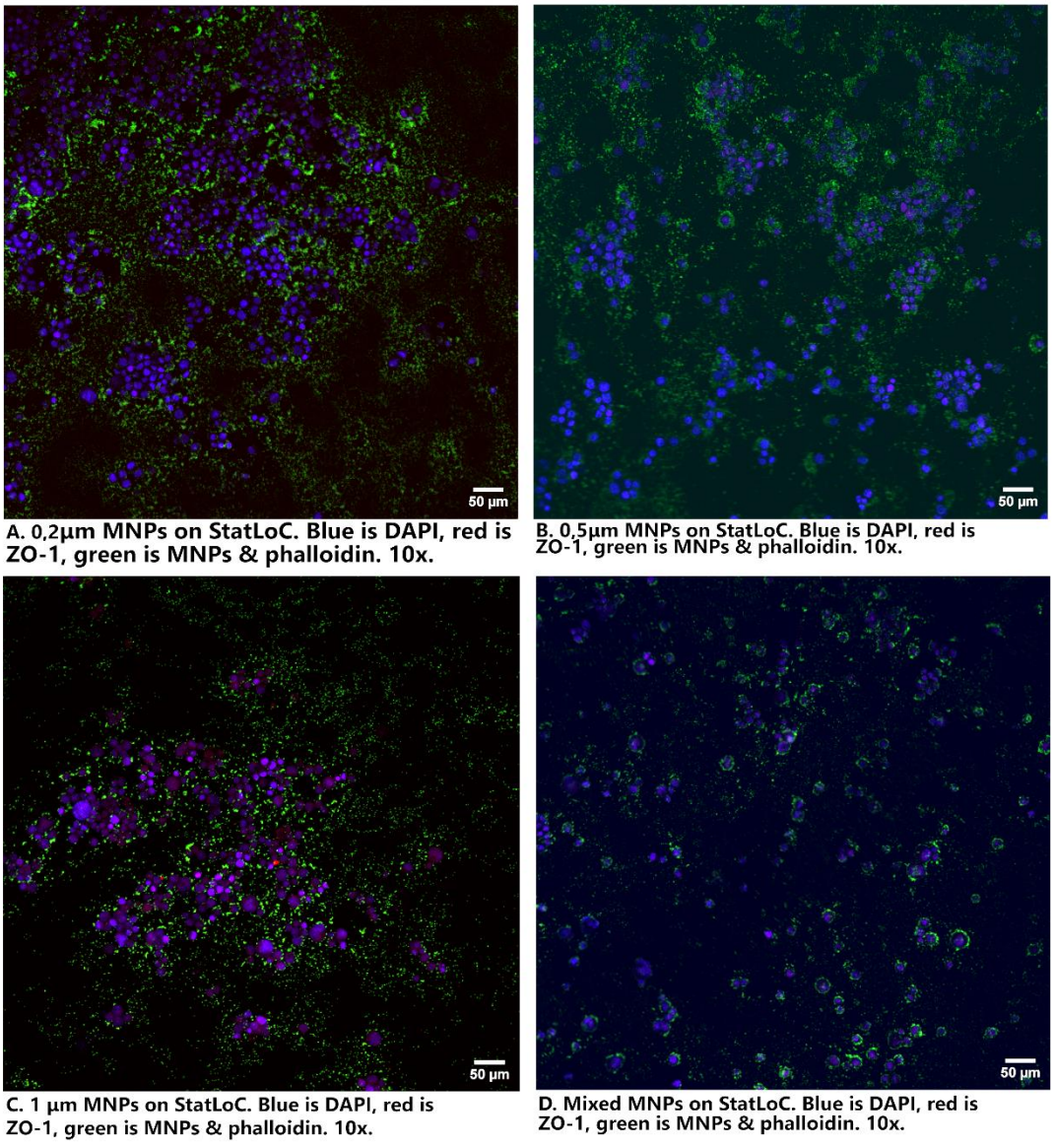

Figure 7: Staining results of the application of MNPs to CaLu-3 cells in StatLoCs. The blue staining is DAPI, the red staining is ZO-1 protein and the green signal are the MNPs and phalloidin. 20x.

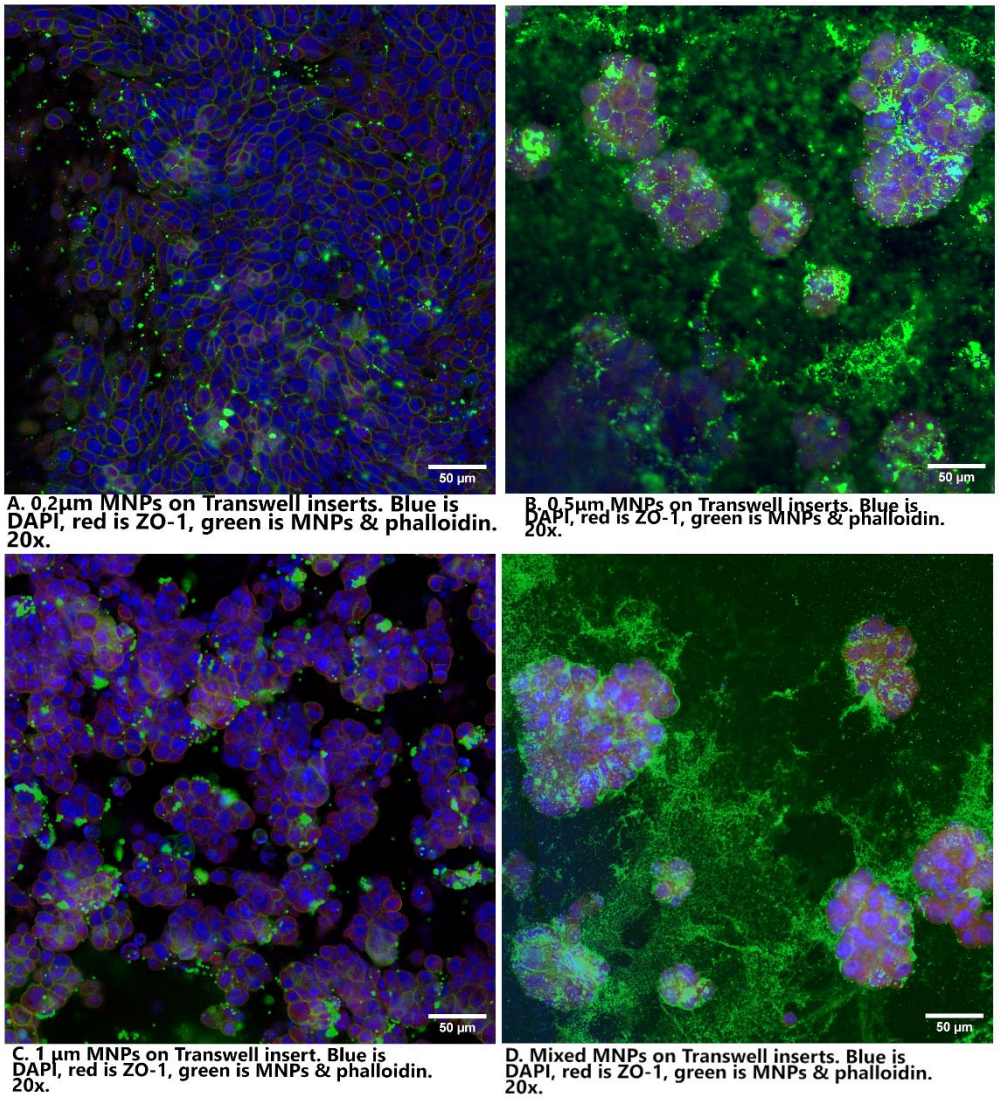

Figure 8: Staining results of the application of MNPs to CaLu-3 cells in Transwells. The blue staining is DAPI, the red staining is ZO-1 protein and the green signal are the MNPs and phalloidin. 20x.

not been reached, while it has been reached in the Transwell inserts. It can also be noted that within the StatLoCs, some areas in the chips are more densely populated with cells than other areas, while this is uniform in the Transwell inserts.

In Figure 5 and Figure 6 the results of the DAPI and ZO-1 protein staining of the Transwells and StatLoCs respectively can be seen, with blue being the nucleus staining DAPI and red being the ZO-1 tight junction protein staining. In Figure 5 both stainings can be seen, with the ZO-1 protein being concentrated in between the cells and the DAPI staining indicating the nuclei. In Figure 6 of the StatLoCs, no ZO-1 protein can be seen in any of the pictures, while the nuclei are indicated in all of them.

In Figure 5 and 6 no notable difference in size or shape of the nuclei can be determined, other than the fact that the Transwell inserts seem to have multiple layers, while the StatLoCs have this in lesser amounts. The StatLoC cells did not succeed in forming a monolayer, while the Transwell cells did. It can be concluded that the Transwell cells contained more ZO-1 protein in comparison to the StatLoCs and in general grew more cells.

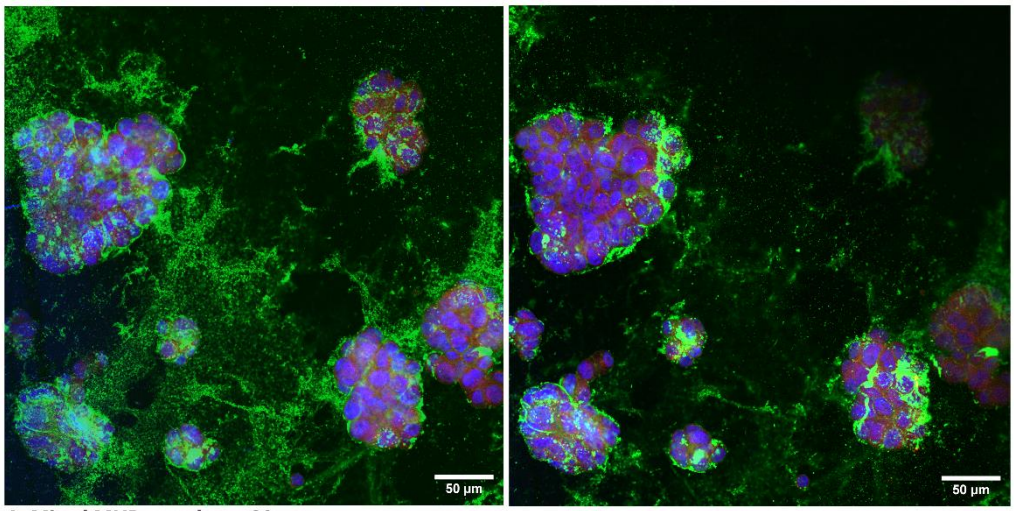

Figure 9: Difference in MNP presence between the top and middle layer of the mixed MNPs in StatLoCs, 20x.

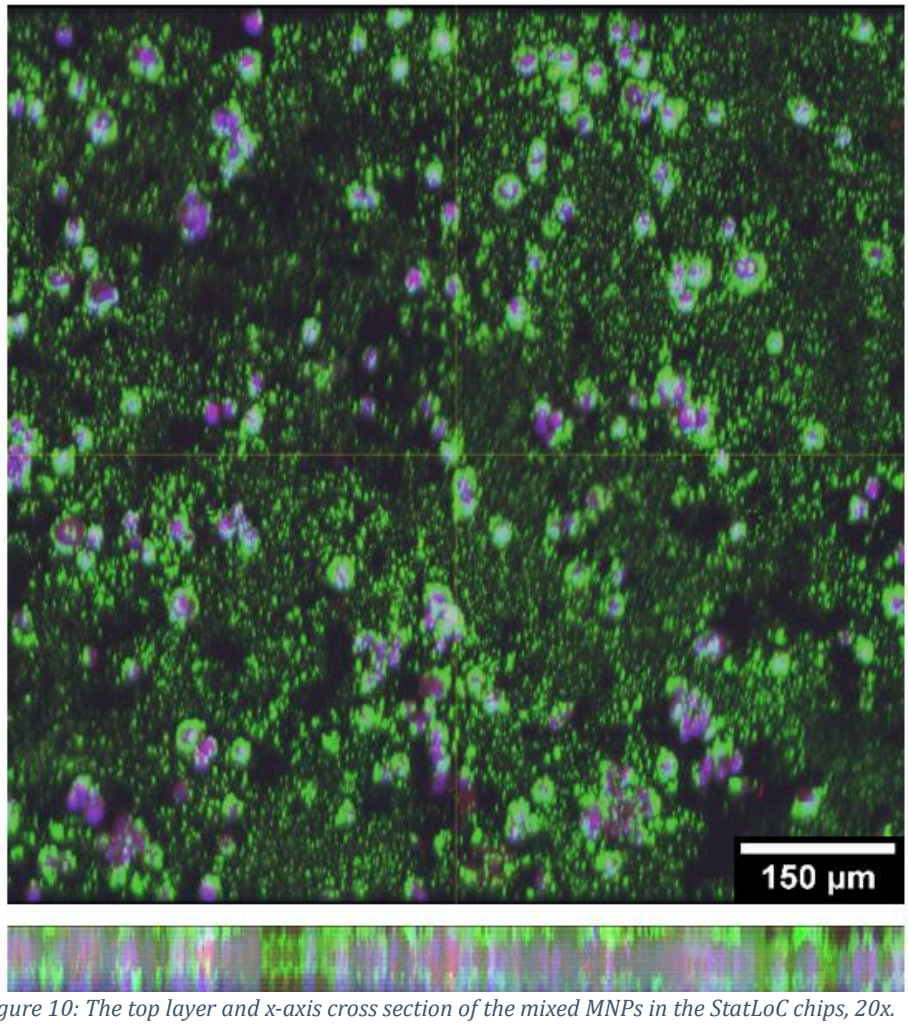

Figure 10: The top layer and x-axis cross section of the mixed MNPs in the StatLoC chips, 20x. The blue staining is DAPI, red is ZO-1 protein and green are the MNPs and phalloidin.

3.4 Uptake studies

The uptake studies are done in order to investigate the translocation and uptake of MNPs in CaLu-3 cells within the StatLoCs and Transwells. Both methods are used to compare differences in uptake and translocation. Some general comparisons between the StatLoC and Transwell inserts is that the Transwell insert cells have started to form layers, while the StatLoC cells are grouped together in small islands within the culture chamber. Another thing of note is that most of the GelMA that was situated in

the StatLoCs has disappeared, with only some chips containing some of the GelMA.

One thing to note when looking at the cells Figure 7 and 8, which show the confocal microscopy results of the StatLoC and Transwell cells respectively, is the difference in nuclei indicated by DAPI. There is an abundance of cells within the Transwells, while there are less within the StatLoCs. The difference in size of the nuclei is also apparent, with the nuclei within the StatLoCs being smaller in comparison to the Transwells. The Transwell nuclei are also more stretched than the StatLoC cells.

The staining of the phalloidin protein is differentiated from the MNPs by its shape, as the MNPs show up like dots and the phalloidin shows up as strands.

From the confocal microscopy results of the StatLoC and Transwell cells it can be noted that there is less phalloidin protein in the StatLoCs than within the Transwells. This can be seen especially well when studying Figure 7 ABD as there are green filaments visible in between and around the cells, which are not visible in the StatLoCs. It also seems that within the StatLoCs, slightly more MNPs are present around the cells. Furthermore, there is less ZO-1 protein to be found within the StatLoC chips in comparison to the Transwell inserts. The location of the ZO-1 protein is the same in both systems, namely in between the cells and in some over the nuclei, resulting in a purple stain.

With regards to the MNPs, these seem to clump to the cell membranes in 80% of the chips. This in turn leads to the MNPs forming larger aggregates. In figure 7 BD, which show the confocal microscopy images for the StatLoC cells, most MNPs are situated around the nuclei. For Figure 8 AC, the cells within the Transwells, this distribution seems to be more disorganised and cell contours are more difficult to distinguish. It can also be observed from Figure 9 that there are less MNPs present in the middle layer in comparison to the top layer of cells.

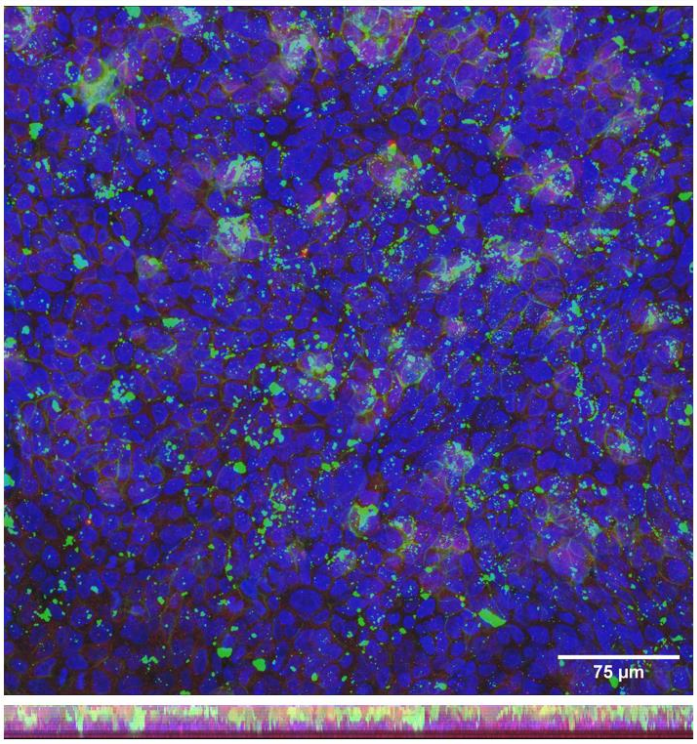

Figure 11: The top layer and x-axis cross section of the 0.2 µm MNPs in a Transwell, 20x. The blue staining is DAPI, red is ZO-1 protein and green are the MNPs and phalloidin.

This is confirmed by cross sections of the cells within the StatLoC and Transwell that can be seen in Figure 10 and 11. The green staining is mostly localized on the apical side of the cells, but MNPs are also situated lower in the cross-section.

The viability of the cells after treatment with the MNPs has been studied with a live/dead staining, of which the results can be found in Figure 13 for cells in the StatLoCs and Figure 12 for cells in the Transwells. A notable difference that can be seen between the StatLoCs and Transwells is the fact that the StatLoC cells show a lot more read staining than the Transwell cells do. However, there is also less staining present within the Transwell cells. In the StatLoC cells, it seems like there is a rising

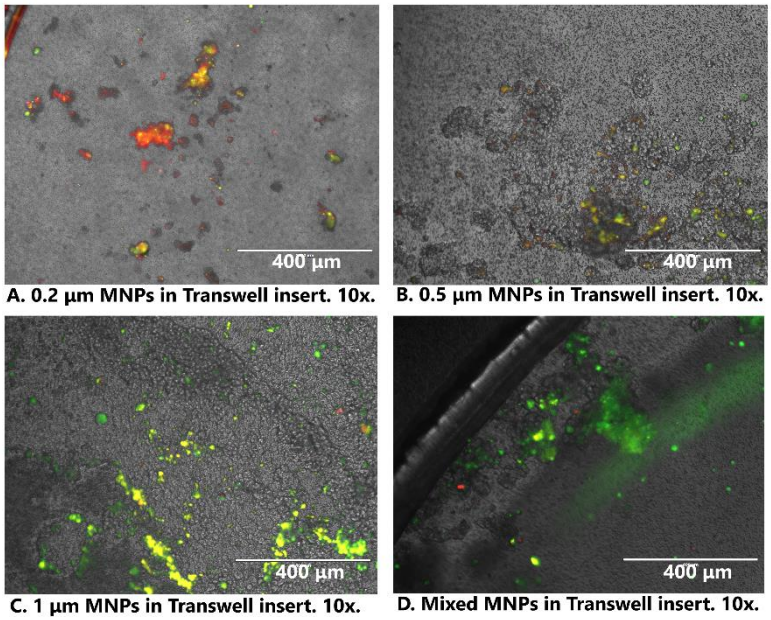

Figure 12: Live/dead staining results performed on Transwells treated with differently size MNPs. Green are the live cells, red are the dead cells, 10x.

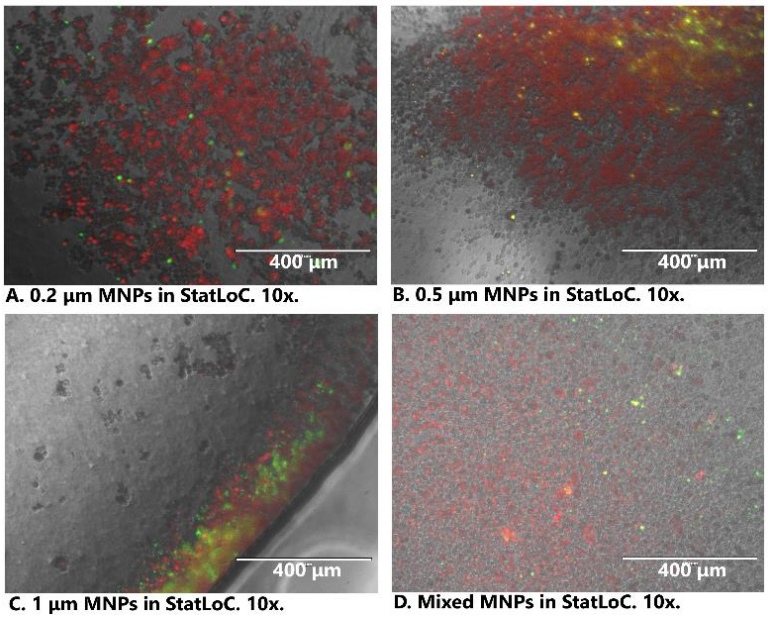

Figure 13: Live/dead staining results performed on StatLoCs treated with differently size MNPs. Green are the live cells, red are the dead cells, 10x.

amount of green staining throughout Figure 12 ABC, which dwindles with the mixed MNPs. For the Transwells this correlation can also be seen, except the cells treated with the mixed MNPs seem to produce more green staining than the StatLoC cells did.

4. Discussion

The experiments described in this paper were performed in a non-optimized system. Therefore, several factors could have influenced the results of this study.

Starting with chip related aspects, when curing the chips in the oven, the protocol indicated to let the chips cure for at least one hour to a maximum of overnight. This means that most chips were cultured for about an hour. During the comparison experiment it was however found out that it is better to let the chip halves cure overnight, as shorter cured PDMS releases more monomers than overnight cured PDMS does. The difference between curing for two hours and curing for overnight is that

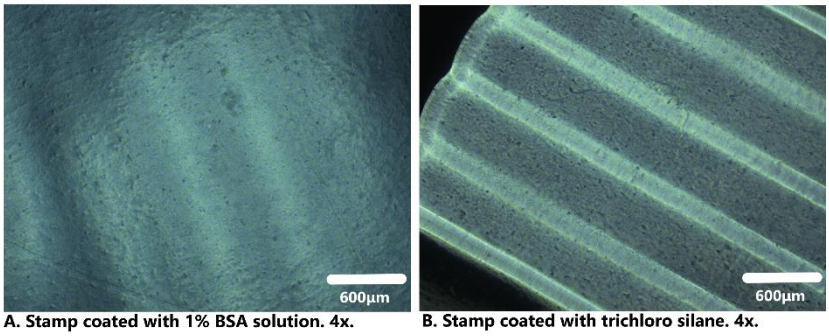

A. Stamp coated with 1% BSA solution. 4x. B. Stamp coated with trichloro silane. 4x.

Figure 14: Difference in the stamp pattern between a stamp coated in 1% BSA solution and a stamp coated with trichloro silane. 4x.

almost twice as much monomers are released when cued two hours in comparison to overnight [12]. One thing to note is that after bonding, most chips were put into the oven again to promote bonding of the halves. This means that the PDMS continued to cure during this, which was often overnight. It is stated that the PDMS monomer have little to no effect on cell proliferation, the little effect being an increase in proliferation dependent on the type of PDMS [12]. However, it is difficult to note what the specific effect has been on the CaLu-3 cells.

Furthermore, during the manufacturing of the static lung-on-chips the bonding was tested on all chips. If not properly bonded, the halves were taken apart and bonded again if the halves were intact. This way, the chips did not leak. However, when conducting the experiments most chips were leaking fluid from the medium channel into the cell culturing well. This made air-liquid interface culturing impossible. In all experiments that use chips, all but one or two chips leaked, which means that ALI culturing did not occur. This has influenced the development of the CaLu-3 cells significantly, as CaLu-3 cells grown at an air-liquid interface are organized in a columnar fashion, develop microvilli and cilia-like structures and are in general more morphologically representative of the lung epithelium in comparison to liquid interface culturing [13]. In future research, a way to prevent this leaking should be researched.

One of the aspects regarding the GelMA that was encountered happened during addition of the GelMA to the StatLoCs. When the BSA coated stamps were placed on top of the uncured gel, air bubbles appeared which created holes in the GelMA. The cells would sink in these holes and thus the cells would not populate the grooves. A solution for this might be to produce the stamp to be more narrow by removing the PDMS margin of the stamp or to make the stamp deeper. Another solution might be to fill the culture chamber with more GelMA so that there is less room for air to remain in the culture chamber.

Another issue with the stamps is that they would stick to the cured GelMA, ripping the created pattern. To try to combat this, two different coatings (1% BSA solution and trichloro silane (Sigma Aldrich)) were used in a separate experiment to determine which would be better to use. As can be seen in Figure 14, the topological grooves made by the stamp with the trichloro silane coating are more visible than the grooves created by the stamps with the BSA coating. The stamp with the trichloro silane coating also had less issues when detaching the stamp from the GelMA. These results suggest that trichloro silane as a coating for the stamps should be explored more in future research, as it shows good potential.

Lastly, during experiments it was noticed that the attachment of the GelMA to the StatLoC-chips deteriorated over the course of the experiments. This meant that the GelMA was not attached to the sides of the cell culturing chamber anymore and would, in the worst case, slide around within the well when the chip was moved. This phenomenon might have been caused by

shrinkage of the GelMA due to liquid being evaporated out of the GelMA. This moving around of the GelMA would not affect the cells if they grew on top of the GelMA. Since the cells mostly preferred to grow on the bottom of the culture chamber, the cells have experienced unnecessary stress. A way to prevent or reduce shrinkage of the GelMA should be researched in order to improve the reliability of the results.

Some factors that were noticed in all performed experiments consist of stress caused by medium removal and monolayers not being present. During medium refreshes, it was noticed that when the medium channels were drained of fluids it would drain the cell culture well too. This caused the cells to experience more mechanical stress than when the medium was drained directly from the well. The effect this stress had on the development on the CaLu-3 cells is difficult to determine. However, it is noted that CaLu-3 monolayers are sensitive to hyperoxia and positive pressure but not to mechanical stress [14]. There are also suggestions that mechanical stresses are necessary for maintaining airway health, which leads to the assumption that the mechanical stress experienced by the cells did not have a significant effect [15].

The last factor that was noted was the absence of monolayers within StatLoCs in all experiments. In the StatLoCs cells were spread very unevenly, with multiple layers being present in some areas while others were empty. A possible cause for this was the GelMA that was added to the bottom of the culture chamber of the StatLoCs, as described above.

From the cell seeding density experiments in section 3.1 and 3.2, it was noted that it is difficult to determine the optimal seeding density. For the well plate there is no truly optimal cell seeding density, as the cells were either overconfluent or not entirely confluent. Hence, it was determined that $3*10^5$ cells/cm^2 is the optimal seeding density in well plates with GelMA at the bottom of the well. To narrow the optimal seeding density down to the correct density, a smaller range was used for the StatLoCs. From this, $4*10^5$ cells/cm^2 and $5*10^5$ cells/cm^2 showed almost identical results in morphology and confluency. To be able to better compare the results of the Transwell inserts and the StatLoCs, the cell seeding density of $5*10^5$ cells/cm^2 was used in further experiments.

Another aspect that might have influenced the results of the seeding density experiment within the well plate is the fact that the GelMA was produced incorrectly. The amount of Irgacure 2959 and gelatin methacryloyl were off by a factor 10, signifying that the GelMA had a lower structural integrity than intended. No notable difference in development of the cells was observed in comparison to development on correctly produced GelMA, thus it is concluded that the cells did not experience detrimental effects due to this error.

When comparing the difference between the Transwells and StatLoCs, it was noted that there was an absence of cell monolayers within the StatLoCs, as described before. The GelMA loosening, fragmenting and moving around in the culture chamber caused the cells to not be able to form a confluent monolayer due to unnecessary mechanical stress.

In the Transwells the GelMA was not present, which is why these cells had a better ability to develop and grow confluent as they did not experience the effects of fragmentation and movement of the GelMA. This can also be seen using Figures 5 and 6, as the nuclei of the StatLoCs are smaller and there is no ZO-1 protein present, thus no tight monolayer has formed. In the Transwells, this protein is present and thus confirms the growth of a tightly bound, confluent monolayer.

The morphology of the cells in the Transwells was as expected and is the same

as the other experiments. The morphology of the cells in the StatLoCs shows a peculiar morphology, as can be seen in Figure 3 FIL. It is unknown how this morphology came to be, but it did not seem to influence other results. Apart from this, the cells in the StatLoCs formed less monolayers and remained smaller than the Transwell cells did.

In the final experiment, it is once again noted that cells cultured in Transwells have a better capability of forming confluent monolayers in comparison to cells cultured in the StatLoCs. However, The Transwells have not formed entirely confluent layers during this experiment either. This occurred because the airlift was performed before the cells formed a confluent layer, which had an impact on the capability to form a monolayer.

Another aspect that might have influenced cell development here is that not only did the GelMA fragment and move, but it shrunk and even broke down in some of the chips. When shrank, the GelMA turned into a sixth of its original size. This was caused by a combination of the water pan of the incubator being empty and the fact that GelMA has enzyme sensitive regions, which may have accelerated the degradation of the GelMA [16].

In the final experiment it was noted that the StatLoC cells were spread further apart in smaller island while the Transwells cells formed sheets, as was observed with the comparison of StatLoCs and Transwell inserts. Despite this, some StatLoC cells still managed to produce some ZO-1 protein, suggesting that these islands were at least tightly clumped together. However, the little ZO-1 protein that was produced within the StatLoCs is trumped by the production within the Transwells, where the ZO-1 protein is present in most inserts in between the cells. This suggests that CaLu-3 cells have a better capability to form tightly interconnected monolayers within Transwell inserts than in StatLoCs, but it is possible for the cells to produce ZO-1 protein within StatLoCs. The difference in this staining can be attributed to the difference in the formation of a monolayer between the different systems.

As for the MNPs, they tend to form larger aggregates which might hinder uptake of the plastics. Particles tend to not be taken up into the cells the larger the particle is, which indicates that the formation of aggregates is lowering the potential of cell damage from taking up MNPs [17]. The plastics also seem to have a limited ability to penetrate into multilayers of cells, as evidenced by figure 9 where there are less MNPs in the middle layers in comparison to the top layer. It is difficult to say which MNP size has penetrated deeper into the layers and if they have been taken up into the cells. In Figure 8 some MNPs can be seen near the nucleus within the membrane, but this can also mean that the MNPs are positioned on top of the cells instead of inside. When comparing this to the results seen in Figure 10 and 11, it is indeed confirmed that most MNPs are stationary on the top layer, but some MNPs also managed to migrate to lower areas. It is however still difficult to say whether they are inside the cells or in between the cells. Lastly, the cells seem to stick to the cell membrane instead of translocating into the cells. This seems to differ within the MNP sizes, as in Figure 12 and 13 there is more red staining in the devices with 0.2 μm MNPs than the 1 μm MNPs.

There are two general improvements that could be made to the MNPs to better represent the in vivo situation. While there are MNPs that are shaped like spheres, there are also other shapes like fibers, films and fragments [4]. Utilization of the different types of MNPs will yield more reliable results. The application of the MNPs should also be improved upon, as it is not realistic for the MNPs to come into contact with the lung epithelial through inhaled fluids. To better stimulate airborne particles, a system that can deposit airborne particles suspended in air is recommended for use.

One example of such system is the Electrostatic Aerosol in Vitro Exposure System [18].

What is interesting within the viability tests is that more cells seem to be alive around the edges of the culture chambers in comparison to the middle of the culture chambers. Another interesting observation is that the viability of the cells seems to decline the smaller the MNPs get. This suggests that smaller MNPs have a higher cell damaging potential in comparison to the larger MNPs, which can be explained by the uptake methods of foreign particles by CaLu-3 cells. This is supported by the fact that nanoplastics are small enough to cross membranes by just passive diffusion and endocytic pathways [17].

5. Conclusion

It has been shown that the optimal cell seeding density within the StatLoCs is equal to the optimal cell seeding density within the Transwell system, it being $5*10^5$ cells/cm^2 . It has also been proven that MNPs cling to the cell membranes but have a low potential for penetration into the cells. This potential differs within size, with the greatest potential being 0.2 µm diameter MNPs and the lowest being the 1 µm diameter MNPs. However, the results of this research show that there is still some optimalization to be done before the StatLoC system can provide good and trustworthy results. In comparison to the Transwell system, the StatLoCs failed to create monolayers in the same manner as the Transwell system did, which caused the barrier integrity for the StatLoCs to be low, causing the results of the experiments to be untrustworthy. The most probable cause for this occurrence is the detachment and fragmentation of the GelMA within the StatLoCs.

6. Acknowledgements

While working on this bachelor assignment, I have received a lot of help and support. For this, I would firstly like to thank Prof. Dr. Ir. Séverine Le Gac, Lysanne Mol and Dr. Kerensa Broersen for their helpful feedback and their support throughout the assignment. I would also like to thank everyone from the AMBER research group for being incredibly welcoming and willing to provide aid when requested. Lastly, I would like to acknowledge Bobbie for his emotional support.

7. References

[1] Oberoi IS, Rajkumar P, Das S. Disposal and recycling of plastics. Mater Today Proc 2021;46:7875–80. https://doi.org/10.1016/J.MATPR.2021.02.562.

[2] Rodrigues ACB, de Jesus GP, Waked D, Gomes GL, Silva TM, Yariwake VY, et al. Scientific Evidence about the Risks of Micro and Nanoplastics (MNPLs) to Human Health and Their Exposure Routes through the Environment. Toxics 2022;10. https://doi.org/10.3390/TOXICS10060308.

[3] Gruber ES, Stadlbauer V, Pichler V, Resch-Fauster K, Todorovic A, Meisel TC, et al. To Waste or Not to Waste: Questioning Potential Health Risks of Micro- and Nanoplastics with a Focus on Their Ingestion and Potential Carcinogenicity. Exposure and Health 2022 15:1 2022;15:33–51. https://doi.org/10.1007/S12403-022-00470-8.

[4] Marrone A, La Russa MF, Randazzo L, La Russa D, Cellini E, Pellegrino D. Microplastics in the center of mediterranean: Comparison of the two calabrian coasts and distribution from coastal areas to the open sea. Int J Environ Res Public Health 2021;18. https://doi.org/10.3390/IJERPH182010712.

[5] Lai H, Liu X, Qu M. Nanoplastics and Human Health: Hazard Identification and Biointerface. Nanomaterials 2022;12. https://doi.org/10.3390/NANO12081298.

[6] Lee Y, Cho J, Sohn J, Kim C. Health Effects of Microplastic Exposures: Current Issues

and Perspectives in South Korea. Yonsei Med J 2023;64:301. https://doi.org/10.3349/YMJ.2023.0048.

[7] Åberg C. Quantitative analysis of nanoparticle transport through in vitro blood-brain barrier models. Tissue Barriers 2016;4. https://doi.org/10.1080/21688370.2016.1143545.

[8] Lust RM. The Pulmonary System. XPharm: The Comprehensive Pharmacology Reference 2007:1–6. https://doi.org/10.1016/B978-008055232-3.60307-1.

[9] Baptista D, Moreira Teixeira L, Barata D, Tahmasebi Birgani Z, King J, Van Riet S, et al. 3D Lung-on-Chip Model Based on Biomimetically Microcurved Culture Membranes. ACS Biomater Sci Eng 2022;8:2684–99. https://doi.org/10.1021/ACSBIOMATERIALS.1C01463/ASSET/IMAGES/LARGE/AB1C01463_0008.JPEG.

[10] Kreft ME, Jerman UD, Lasič E, Hevir-Kene N, Rižner TL, Peternel L, et al. The characterization of the human cell line Calu-3 under different culture conditions and its use as an optimized in vitro model to investigate bronchial epithelial function. European Journal of Pharmaceutical Sciences 2015;69:1–9. https://doi.org/10.1016/J.EJPS.2014.12.017.

[11] Miranda I, Souza A, Sousa P, Ribeiro J, Castanheira EMS, Lima R, et al. Properties and Applications of PDMS for Biomedical Engineering: A Review. J Funct Biomater 2022;13. https://doi.org/10.3390/JFB13010002.

[12] Carter S-SD, Atif A-R, Kadekar S, Lanekoff I, Engqvist H, Varghese OP, et al. PDMS leaching and its implications for on-chip studies focusing on bone regeneration applications. Organs-on-a-Chip 2020;2:100004. https://doi.org/10.1016/J.OOC.2020.100004.

[13] Grainger CI, Greenwell LL, Lockley DJ, Martin GP, Forbes B. Culture of Calu-3 cells at the air interface provides a representative model of the airway epithelial barrier. Pharm Res 2006;23:1482–90. https://doi.org/10.1007/S11095-006-0255-0/FIGURES/3.

[14] Zhu Y, Chidekel A, Shaffer TH. Cultured Human Airway Epithelial Cells (Calu-3): A Model of Human Respiratory Function, Structure, and Inflammatory Responses. Crit Care Res Pract 2010;2010:1–8. https://doi.org/10.1155/2010/394578.

[15] Button B, Boucher RC, Group TU of NCVL. Role of Mechanical Stress in Regulating Airway Surface Hydration and Mucus Clearance Rates. Respir Physiol Neurobiol 2008;163:189. https://doi.org/10.1016/J.RESP.2008.04.020.

[16] Zhu M, Wang Y, Ferracci G, Zheng J, Cho NJ, Lee BH. Gelatin methacryloyl and its hydrogels with an exceptional degree of controllability and batch-to-batch consistency. Scientific Reports 2019 9:1 2019;9:1–13. https://doi.org/10.1038/s41598-019-42186-x.

[17] Gigault J, El Hadri H, Nguyen B, Grassl B, Rowenczyk L, Tufenkji N, et al. Nanoplastics are neither microplastics nor engineered nanoparticles. Nature Nanotechnology 2021 16:5 2021;16:501–7. https://doi.org/10.1038/s41565-021-00886-4.

[18] De Bruijne K, Ebersviller S, Sexton KG, Lake S, Leith D, Goodman R, et al. Design and Testing of Electrostatic Aerosol In Vitro Exposure System (EAVES): An Alternative Exposure System for Particles. Inhal Toxicol 2009;21:91–101. https://doi.org/10.1080/08958370802166035.